

THE CALIFORNIA-KEPLER SURVEY. V.  
PEAS IN A POD: PLANETS IN A KEPLER MULTI-PLANET SYSTEM ARE SIMILAR IN SIZE AND  
REGULARLY SPACED <sup>1</sup>LAUREN M. WEISS<sup>2,3,11</sup>, GEOFFREY W. MARCY<sup>4</sup>, ERIK A. PETIGURA<sup>5,12</sup>, BENJAMIN J. FULTON<sup>6,13</sup>, ANDREW W. HOWARD<sup>5</sup>, JOSHUA N. WINN<sup>7</sup>, HOWARD T. ISAACSON<sup>4</sup>, TIMOTHY D. MORTON<sup>7</sup>, LEA A. HIRSCH<sup>4</sup>, EVAN J. SINUKOFF<sup>6,14</sup>, ANDREW CUMMING<sup>2,8</sup>, LESLIE HEBB<sup>9</sup>, AND PHILLIP A. CARGILE<sup>10</sup><sup>1</sup>Based on observations obtained at the W. M. Keck Observatory, which is operated jointly by the University of California and the California Institute of Technology. Keck time has been granted by the University of California, and California Institute of Technology, and the University of Hawaii.<sup>2</sup>Institut de Recherche sur les Exoplanètes, Montréal, QC H3T 1J4, Canada<sup>3</sup>Université de Montréal, Montréal, QC H3T 1J4, Canada<sup>4</sup>University of California at Berkeley, Berkeley, CA 94720, USA<sup>5</sup>California Institute of Technology, Pasadena, CA 91125, USA<sup>6</sup>Institute for Astronomy, University of Hawaii at Manoa, Honolulu, HI 96822, USA<sup>7</sup>Princeton University, Princeton, NJ 08544, USA<sup>8</sup>McGill University, Montréal, QC H3A 0G4, Canada<sup>9</sup>Hobart and William Smith Colleges, Geneva, NY 14456, USA<sup>10</sup>Harvard-Smithsonian Center for Astrophysics, 60 Garden St, Cambridge, MA 02138, USA<sup>11</sup>Trottier Fellow<sup>12</sup>Hubble Fellow<sup>13</sup>NSF Graduate Research Fellow<sup>14</sup>Natural Sciences and Engineering Research Council of Canada Graduate Student Fellow

## ABSTRACT

We have established precise planet radii, semi-major axes, incident stellar fluxes, and stellar masses for 909 planets in 355 multi-planet systems discovered by *Kepler*. We find that planets within a single multi-planet system tend to be closer in size than planets drawn randomly from the collection of multi-planet systems. This is true even when considering systems with similar host stars; we find, at most, a weak correlation between planet radius and stellar mass. Evidently, it is not the stellar mass but some other property or process that enforces the similarity of planet sizes. When adjacent planets in a multi-planet system are not similar in size, the inner planet is smaller in  $65 \pm 6\%$  of cases. The tendency for the inner planet to be smaller is especially pronounced when the inner planet has a short period ( $\lesssim 10$  days) or equivalently, high radiation flux ( $\gtrsim 150$  times the Earth's insolation). This could be the result of photoevaporation. We also find that adjacent planets within a given system tend to be spaced in a regular geometric progression, with a typical semi-major axis ratio of 1.5. Using empirical mass-radius relationships, we estimate the mutual Hill separations of planet pairs. We find that 93% of the planet pairs are at least 10 mutual Hill radii apart, and that a spacing of 10-30 mutual Hill radii is most common.

*Keywords:* catalogs, surveys, planetary systems, stars

## 1. INTRODUCTION

Multi-planet systems provide a fossil record of the physics that drive planet formation. The *Kepler* Mission (Borucki et al. 2010) has enabled detailed statistics of hundreds of coplanar multi-planet systems (Latham et al. 2011; Lissauer et al. 2011; Lissauer et al. 2012; Fabrycky et al. 2014; Lissauer et al. 2014; Rowe et al. 2014). In the *Kepler* multi-planet systems, multiple

planets transit the star, resulting in measured orbital periods and planet-to-star radius ratios for each transiting planet. The observed and statistically inferred orbital properties in multi-planet systems have been used to deduce possible planet formation histories (Fang & Margot 2012; Hansen & Murray 2013; Steffen & Hwang 2015; Pu & Wu 2015; Ballard & Johnson 2016; Xie et al. 2016).

Until recently, the stellar properties in the population of *Kepler* multi-planet systems were poorly understood. The majority of these stars had only photometric characterization via the Kepler Input Catalog (KIC, [Brown et al. 2011](#)). The uncertainties inherent in broad pass-band stellar characterization resulted in uncertainties of 16% in the stellar masses and 42% in the stellar radii, on average ([Mullally et al. 2015](#); [Johnson et al. 2017](#)).

With the goal of clarifying the stellar and planetary properties of *Kepler*’s multi-planet systems, the California Kepler Survey (CKS) determined precise stellar and planetary properties for 355 *Kepler* multi-planet systems containing 909 transiting planets. [Petigura et al. \(2017, CKS I\)](#) presented the host star spectra and their observational properties  $T_{\text{eff}}$ ,  $\log g$ ,  $[\text{Fe}/\text{H}]$ , and  $v \sin i$ . These observed quantities were converted to physical stellar parameters  $M_*$ ,  $R_*$ , and age using stellar evolutionary models ([Johnson et al. 2017, CKS II](#)). The improved stellar characterization results in a median uncertainty of 5% in the stellar mass and 10% in the stellar radius.

With improved stellar parameters, it is possible to improve the characterization of planets as well. In CKS II, the updated stellar parameters were used to compute planetary radii, semi-major axes, and equilibrium temperatures for the planets these stars. The improved stellar and planetary parameters enable a more accurate and precise characterization of the multi-planet systems than was previously available.

In this paper, we examine several properties of *Kepler*’s multi-planet systems that are clarified by the improved stellar parameters. In section 2 we describe how the multi-planet systems analyzed herein were selected. In section 3 we show that the planetary sizes are related within multi-planet systems, with attention to how stellar mass and the incident stellar flux correlate with planet sizes. In section 4 we show that the planet semi-major axis ratios are strongly peaked at a value of 1.5. Using the updated planet radii and semi-major axes, we employ empirical mass-radius relationships to compute the pairwise mutual Hill separations for the multis. We conclude in section 5.

## 2. THE SAMPLE

The initial set of CKS systems with multiple transiting planet candidates consists of 469 stars with at least two transit-like signals, and a total of 1215 transit-like signals that were at one time flagged as Kepler Objects of Interest (KOIs). From these, we discarded the known false positives, removing 59 non-planetary signals as determined in CKS I. We then discarded stars that were diluted by at least 5% by a second star in the *Kepler* aperture (as determined in the stellar companion catalog of [Furlan et al. 2017](#)), removing 30 stars hosting

69 planet candidates. We discarded planets for which [Mullally et al. \(2015\)](#) measured  $b > 0.9$ , for which the high impact parameters adversely affected our ability to determine accurate planet radii, removing 75 planet candidates. We removed planets for which the measured signal-to-noise ratio (SNR) was less than 10 since these planets have poorly determined radii and impact parameters, removing 48 planet candidates. Finally, we discarded systems that have been reduced to one valid planet candidate (55 systems). After these cuts, our sample of “CKS multis” contained 909 high-purity planet candidates, which we henceforth call planets, in 355 multi-planet systems.

Figure 1 shows the architectures of CKS systems with at least 4 transiting planets. Each row corresponds to one planetary system. The systems are ordered by stellar mass, which is listed to the right of each system. Several architectural features emerge: (1) the size of one planet in a system is a good predictor of the sizes of other planets in the same system, (2) the spacing between a pair of planets in a system is a good predictor of the spacing of additional planets in that same system, (3) the stellar mass does not appear to be a good predictor of planet sizes, (4) when planets are not the same sizes, the inner planets are usually smaller. Below, we quantitatively investigate these observations.

## 3. PLANETS IN THE SAME SYSTEM HAVE SIMILAR SIZES

To quantify whether the planets in a multi-planet system have preferentially similar sizes, we performed the following experiment. In each multi-planet system, we took the ratio of the planet radii for each pair of adjacent planets in the system. (We did not consider non-adjacent pairs because these do not give independent information.) For each adjacent planet pair, we asked whether the smaller planet could have been detected at the longer orbital period. To compute detectability, we calculated the expected signal-to-noise (SNR) of a planet with size  $R_p$  and orbital period  $P$  for a star with bulk density  $\rho_*$ , radius  $R_*$ , and 6-hour Combined Differential Photometric Precision (CDPP<sub>6h</sub>, a measure of the stellar photometric noise over 6 hours, [Christiansen et al. 2012](#)) using:

$$\text{SNR} = \frac{(R_p/R_*)^2 \sqrt{3.5\text{yr}/P}}{\text{CDPP}_{6h} \sqrt{6\text{hr}/T}} \quad (1)$$

$$T = 13\text{hr}(P/1\text{yr})^{1/3}(\rho_*/\rho_\odot)^{-1/3} \quad (2)$$

If the smaller planet, when placed at the larger orbital period, produced  $\text{SNR} > 10$ , the observed planet radius ratio was included in our sample of the real distribution of planet size ratios. This yielded 502 ratios of adjacent planet radii, which are shown in Figure 2.

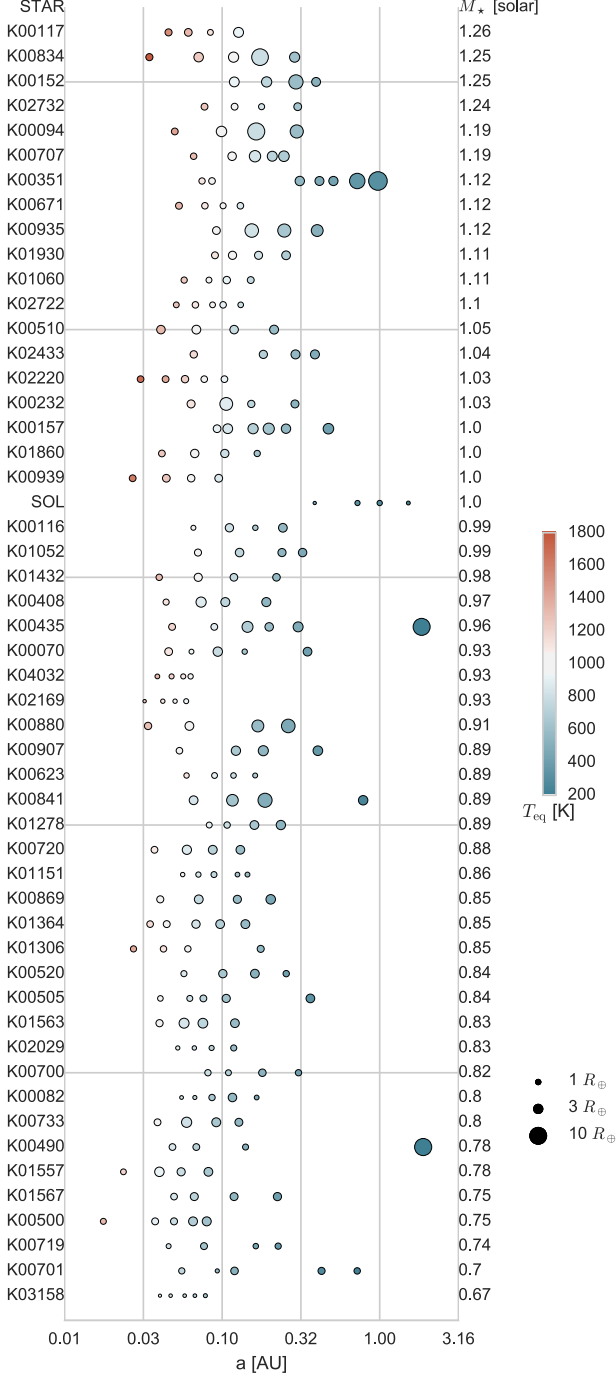


**Figure 1.** Architectures of CKS multis with at least 4 transiting planets. Each row corresponds to one planetary system (name on y-axis) and shows the planet semi-major axes (x-axis; note the log scale). The point sizes correspond to the planet radii, and the point colors correspond to the equilibrium temperatures (see key to the right). The systems are ordered by stellar mass, which is listed to the right of each system. The inner solar system is included for comparison.

To construct a control sample, we did the following:

1. For each star, construct an artificial planetary system by randomly drawing (with replacement) planet radii from the observed distribution of planet radii in the multis. The number of planets in the artificial system is set equal to the number of actual planets detected around that star.
2. Compute the adjacent planet ratios in this artificial planetary system in the same manner as within a true planetary system. (Only include the pairs of planets in which the smaller planet would be detectable at the longer orbital period.)
3. Repeat 1000 times for each star.

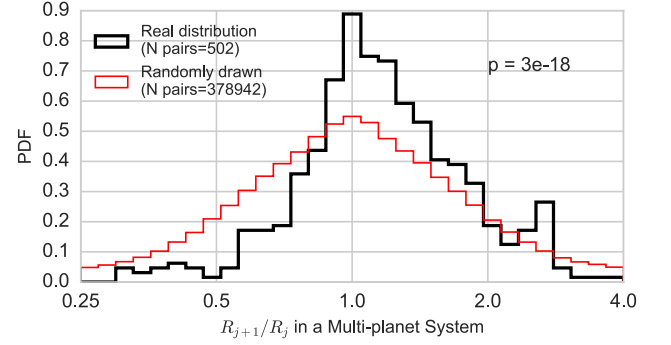


**Figure 2.** The ratios of adjacent planet sizes within the same multi-planet system (black line) compared to a control sample of artificial systems constructed by drawing from the radii of the transiting multis at random (red line). In both the real and the random distributions, pairs are only counted if the smaller planet in the pair is detectable at the longer orbital period. The  $p$ -value of a K-S test comparing the real vs. random distributions of planet radius ratios is shown; with a confidence of  $> 99.9\%$ , we can rule out the hypothesis that these two populations come from the same underlying distribution. The distribution of real planet radius ratios is significantly more peaked at 1.0 than the randomly drawn distribution, indicating that planets in the same system are preferentially the same sizes. When planets in a real system are not the same size, the inner planet is usually the smaller planet (in  $65 \pm 6\%$  of pairs).

Figure 2 compares the real and artificial distributions for the ratios of planet radii. Using a Kolmogorov-Smirnov (K-S) test, we found a  $p$ -value of  $< 0.001$ , allowing us to conclude with  $> 99.9\%$  confidence that the real planet radius ratios are not drawn from the same distribution as our randomly drawn ratios. *In other words, if we know the size of one planet in a multi-planet system, we can make a better-than-random prediction about the sizes of other planets in the system.* In particular, the real distribution has a much sharper peak at a planet size ratio of 1.0 than the artificial distribution, meaning that planets in multi-planet systems are more

likely to be similarly sized to each other than what we would expect drawing their sizes at random.

One source of uncertainty in comparing the real distribution of planet radius ratios with the control sample is that stellar radius uncertainties play a role in the construction of the control sample, broadening it slightly, whereas the stellar radius uncertainty has no effect on the comparison of planets within the same system. To test the effect of the stellar uncertainty on our comparison, we constructed a smeared distribution of the real planet ratios. In each system, we perturbed each planet radius by the fractional uncertainty in the stellar radius, and then drew planet ratios. The broadening of the distribution of real planet ratios was insignificant (6%) compared to the discrepancy between the real planet ratios and the control sample (65%).

How do planets know to be the same size? Perhaps some feature of their environment sculpts the sizes of planets. Below, we examine how stellar mass and stellar incident flux affect the planet size distribution.

### 3.1. Stellar mass and planet size in *Kepler*’s multis

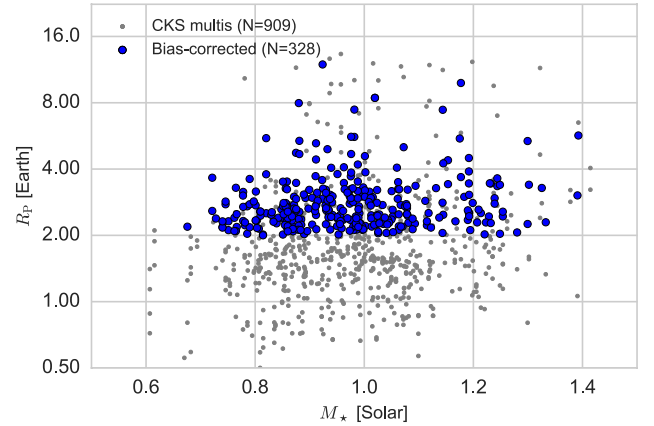
We examine whether stellar mass correlates with planet size in a way that generates the self-similarity of planets in the same system. Are the planets conforming to a size that is determined by the host star?

Figure 3 shows how planet radius varies with stellar mass in the *Kepler* multiplanet systems. Among the 909 CKS multis, there is a rising floor of planet radius with increasing stellar mass that is probably related to a known selection bias: it is easier to find a small planet around a small star (a low-mass star) than a large star (often a high-mass star), and so the minimum detectable planet size is correlated with stellar mass. To counter this selection bias, we selected a subsample of stars for which a planet with  $R_p > 2 R_\oplus$  and  $P < 50$  days was detectable (according to equation 1) with  $\text{SNR} > 10$ , and then restricted the planets to  $R_p > 2 R_\oplus$  and  $P < 50$  days, thus ensuring that any planet in our subsample was detectable around any star in our subsample with  $\text{SNR} > 10$ .

To investigate a possible correlation between stellar mass and planet size, we used a Pearson-R correlation test. The Pearson-R test yielded a correlation of 0.13 with a significance of 0.016, indicating a possible slight correlation between stellar mass and planet radius. However, when we restricted the planets to have  $R_p < 4 R_\oplus$ , the p-value increased to 0.03. This means that for CKS multis between 2 and 4  $R_\oplus$  with  $P < 50$  days, we cannot reject the null hypothesis that there is no correlation between stellar mass and planet radius. We repeated this test using different maximum orbital periods (30, 50, 100, and 200 days) and a different range of radii (1.5  $R_\oplus$  to 4  $R_\oplus$ ). In each of these combinations,

we found at most a weak, low-significance correlation between planet size and stellar mass. The strength of the Pearson-R correlation ranged from 0.1–0.15, depending on the threshold  $R_p$  and  $P$  chosen to construct a bias-corrected sample. These correlation values are low, indicating that the scatter in planet size at a given stellar mass dominates over the slight upward trend. Thus, some physical property other than the stellar mass is important in setting the sizes of the planets.

We performed a similar analysis for stellar metallicity and also found no strong trend. More details about how stellar metallicity correlates with planet radius will be discussed by Petigura et al. (in preparation).



**Figure 3.** Planet radius versus stellar mass. Among the full sample of CKS multis (gray), there is a selection bias: small planets are easy to detect around small stars (which are also low-mass stars), whereas small planets are much harder to detect around large stars (which are often high-mass stars). Therefore, we identify a “bias-corrected” subsample of stars and planets (blue) for which any planet in the subsample is detectable with  $\text{SNR} > 10$  around any other star in the subsample. The planets in the bias-corrected subsample satisfy  $R_p > 2 R_\oplus$  and  $P < 50$  days; and a planet of  $2.0 R_\oplus$  at 50 days is detectable around all the stars in the subsample. In the bias-corrected subsample, a Pearson-R correlation test between the stellar mass and planet radius yields a value of 0.14 with a significance of 0.016, indicating that there is at most a slight correlation between stellar mass and planet radius.

### 3.2. Incident Stellar Flux correlates with planet size ratios

Although multi-planet systems often form planets of similar sizes, sometimes there is size diversity in a system. In Figure 2, the outer planet of the pair is larger  $65 \pm 6\%$  of the time. (The uncertainty is dominated by Poisson statistics of 6%, not the intrinsic uncertainties in planet radii, which create an uncertainty of 0.4%.) We investigate whether incident stellar flux is correlated with the asymmetry of planet sizes.

We extracted two subsamples from the distribution of planet pairs: one in which the adjacent planets straddle

the line of  $150\times$  Earth’s insolation ( $F_{\oplus}$ , such as the historic Kepler-36 b and c, [Carter et al. 2012](#)), and one in which both planets receive less than  $150 F_{\oplus}$  (Figure 4). For adjacent planet pairs that straddle  $150 F_{\oplus}$ , the inner planet is the smaller planet in  $74\pm 9\%$  of pairs. For adjacent pairs in which both planets receive less than  $150 F_{\oplus}$ , the asymmetry between the inner and outer planet sizes is less pronounced: the inner planet is smaller in only  $58\pm 8\%$  of pairs.

We repeated this experiment with different thresholds for the incident flux ( $300 F_{\oplus}$  and  $50 F_{\oplus}$ ) and also found that the inner planet is usually smaller, with approximately the same significance. We also repeated this experiment using only planets smaller than  $4 R_{\oplus}$ , and the result was unchanged.

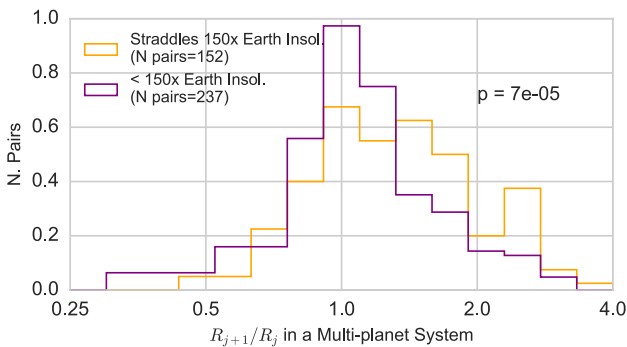


**Figure 4.** The planet radius ratio distributions for planet pairs that straddle an incident stellar flux of  $150 F_{\oplus}$  (orange), and the radius ratios for planet pairs in which both planets receive less than  $150 F_{\oplus}$  (purple). In both distributions, pairs are only counted if the smaller planet in the pair is detectable at the longer orbital period. The K-S test significance comparing the two real distributions is shown; with a confidence of  $> 99.9\%$ , we can rule out the hypothesis that these two populations come from the same underlying distribution. Among the planet pairs that straddle  $150 F_{\oplus}$ , the center of the distribution is at a higher value of  $R_{j+1}/R_j$ , meaning the outer planet tends to be larger than the inner planet.

#### 4. PLANETS HAVE REGULAR SPACINGS

From Figure 1, we hypothesize that planets have regular spacings. We explore several ways of quantifying the distribution of planet spacings below.

##### 4.1. Semi-major Axes

To quantify whether the planets in a multi-planet system have regular spacings, we performed an experiment that is shown in Figure 5. Our procedure was very similar to what is described above. Within each real multi-planet system, we computed the ratio of adjacent planet radii, only counting the pair if the smaller planet could have been detected at the larger orbital period. Then, to construct an artificial distribution of planet

pairs, we drew semi-major axis values at random from the observed population of multis. We sorted the planets in order of semi-major axis and computed the ratio of their semi-major axes. To avoid situations in which the randomly drawn planets were too close to each other for plausible stability, we rejected pairs that were closer than 10 mutual Hill radii<sup>1</sup>.

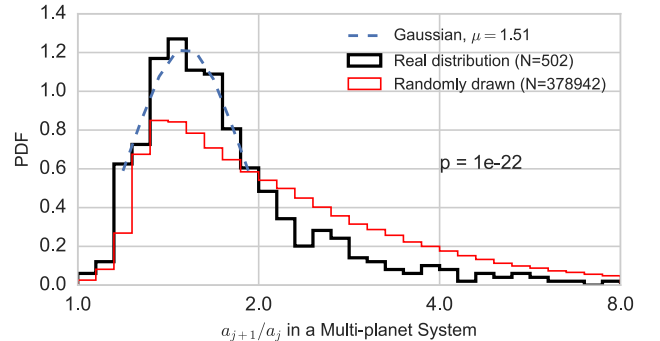


**Figure 5.** The ratios of adjacent planet semi-major axes within a multi-planet system (black line) compared to a control sample of artificial systems constructed by drawing the semi-major axes of the transiting multis at random and discarding any pairs closer than 10 mutual Hill radii (red line). In both the real and random distributions, pairs are only counted if the smaller planet is detectable at the longer orbital period. The number of real planet pairs and the K-S test significance are shown. The real distribution is peaked at  $a_2/a_1 = 1.5$ , i.e.  $P_{j+1}/P_j = 1.8$ , whereas the randomly drawn distribution is relatively smooth. The preferential spacing of planets in multi-transiting systems can be used as a tool for predicting the orbits of additional, yet-undetected planets in the system.

We find that the distribution of ratios of adjacent planet semi-major axes in real multi-planet systems is peaked at 1.5, whereas the artificially constructed distribution is less peaked. Fitting a Gaussian to the distribution of  $\log(a_{j+1}/a_j)$  near the peak (PDF  $> 0.6$ ), we identified a peak corresponding to  $a_{j+1}/a_j = 1.5 \pm 0.2$ . Thus, given a planet in a multi-planet system at semi-major axis  $a_j$ , we would be doing better than a random guess if we predicted that the next planet was at  $a_{j+1}/a_j = 1.5$ .

Uncertainties in the stellar masses contribute extra noise ( $\sim 6\%$ ) to the histogram of orbital distance ratios, but this is negligible in comparison to the observed difference between the artificial and real distributions.

We also did this analysis comparing the orbital period (instead of semi-major axis) for adjacent planets. The peak was broader:  $P_{j+1}/P_j = 1.8 \pm 0.3$ .

##### 4.2. Planets are 20 Mutual Hill Radii Apart

<sup>1</sup> See the next subsection for a definition of the mutual Hill radius.



Planets communicate with their neighbors through gravitational interactions. To better understand the typical spacing between planets, we considered the separation between a pair of planets in terms of their gravitational influence, of which the mutual Hill radius is the natural unit. The mutual Hill radius of two planets of masses  $m_j$  and  $m_{j+1}$  orbiting a star of mass  $M_\star$  at semi-major axes  $a_j$  and  $a_{j+1}$  is

$$R_H = \left( \frac{m_j + m_{j+1}}{3M_\star} \right)^{1/3} \frac{(a_j + a_{j+1})}{2} \quad (3)$$

and the separation between two planets, in units of mutual Hill radii, is

$$\Delta = (a_{j+1} - a_j)/R_H \quad (4)$$

(Gladman 1993).

To compute planet separations in mutual Hill radii, it is necessary to assume planet masses. We converted our precise planet radii to estimates of planet masses ( $M_p$ ) and densities ( $\rho_p$ ) via the empirical mass-radius relationships of Weiss & Marcy (2014) and Weiss et al. (2013):

$$R_p/R_\oplus < 1.5 :$$

$$\begin{aligned} \rho_p &= 2.43 + 3.39(R_p/R_\oplus) \text{ g cm}^{-3} \\ M_p &= (\rho_p/5.51 \text{ g cm}^{-3})(R_p/R_\oplus)^3 M_\oplus \end{aligned} \quad (5)$$

$$1.5 \leq R_p/R_\oplus \leq 4.0 :$$

$$M_p = 2.69(R_p/R_\oplus)^{0.93} M_\oplus \quad (6)$$

$$4.0 < R_p/R_\oplus < 9.0 :$$

$$M_p = 0.86(R_p/R_\oplus)^{1.89} M_\oplus^{\text{ii}} \quad (7)$$

$$9.0 \leq R_p/R_\oplus :$$

$$M_p = 318 M_\oplus; \text{ i.e., } M_J^{\text{iii}} \quad (8)$$

Although there is large scatter in the planet masses with respect to these mean empirical relations (Marcy et al. 2014; Weiss & Marcy 2014; Rogers 2015; Wolfgang & Lopez 2015; Chen & Kipping 2017), we have no basis for deciding which planets should be higher or lower mass than the mean, and so we adopt a simple one-to-one mapping of radius to mass.

The orbital separations in mutual Hill radii are shown in Figure 6. The CKS multis are shown, as are the sub-

<sup>i</sup> The original formulation of this relation includes a very weak dependence on the incident stellar flux ( $(F/F_\oplus)^{0.057}$ ). Since this weak dependence might not be valid, we apply  $F = 100 F_\oplus$  as a substitute.

<sup>ii</sup> The masses of Jupiter-sized planets vary widely. Because only 5% of the systems host planets in this size range, the results are insensitive to the masses we assume for these planets.

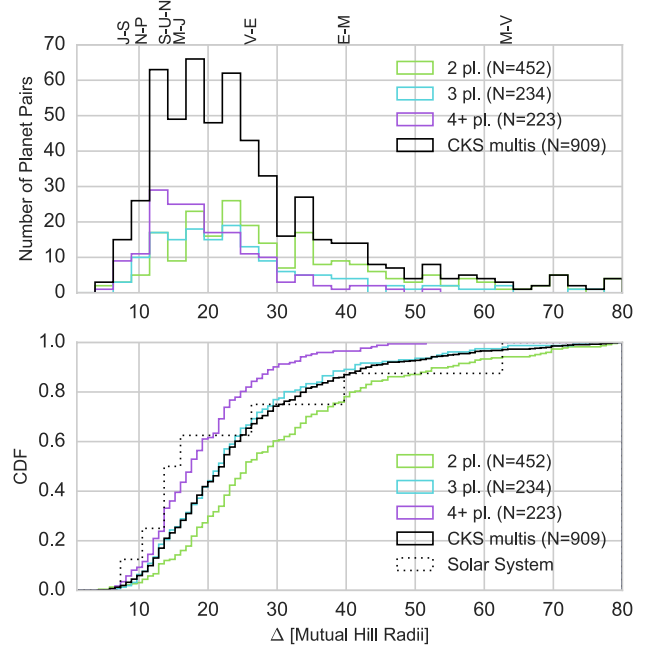


**Figure 6.** Top: Separation in mutual Hill radii between adjacent pairs of transiting planets, assuming the empirical mass-radius relations from Weiss & Marcy (2014) and Weiss et al. (2013). The CKS multis are shown (black line), as are the sub-samples with two (green), three (cyan), or at least four (purple) transiting planets. Planet pairs in the solar system are shown as dotted lines, with the planet names at the top of the plot. Bottom: same as top, but showing the cumulative distribution function.

samples with two, three, or at least four transiting planets. The majority of *Kepler* planets (93%) are at least 10 mutual Hill radii apart. Systems with high multiplicity of transiting planets (4+) tend to have the smallest Hill separations. For systems that have larger Hill separations, it is possible that the eccentricities and/or mutual inclinations of the planets are larger, requiring larger separations between the planets for stability. For systems with pairs of planets more than about 20 mutual Hill radii apart, it is also possible that another planet resides between them, but either does not transit or has not been detected.

In terms of their mutual Hill radii, the *Kepler* systems are quite similar to the solar system. Note that the cumulative distribution function for the solar system in Figure 6 traces the distribution for the CKS multis. (It is difficult to calculate the significance of the similarity because the solar system has only 9 planets.) Although the *Kepler* planetary systems are often distinguished from the solar system using the phrase “dynamically packed,” Figure 6 underscores that in a dynamical sense, their orbital separations are very similar. The orbital separations of the *Kepler* planets in units of a.u. are small compared to the solar system, but this is not so in units

of mutual Hill radii.

## 5. SUMMARY AND DISCUSSION

In this paper, we have found the following observational results among the *Kepler* systems with multiple transiting planets:

1. Planets within a given system are more similar in size than planets drawn randomly from the collection of multi-planet systems.
2. Stellar mass is not strongly correlated with planet sizes.
3. For any two adjacent planets in a single system, the inner planet tends to be smaller than the outer planet. This tendency is strongest when the inner planet receives  $\gtrsim 150$  times the flux Earth receives from the Sun, and the other planet receives less.
4. Planets have a regular geometric spacing, with a typical ratio of 1.5 between the semi-major axes of adjacent planets.
5. Converting planet radii to estimated masses, we find that planets tend to be about 20 mutual Hill radii apart, and are rarely closer together than 10 mutual Hill radii. Their dynamical packing is similar to the solar system.

Our work builds on previous studies of *Kepler* multi-planet systems. [Lissauer et al. \(2011\)](#) also found that planets in multi-planet systems tend to be the same size, but with a much smaller sample of planets in multi-planet systems, resulting in only 71 independent, detectability-corrected ratios. Our work repeats their experiment but with 502 independent, detectability-corrected ratios.

Why are planets in a multi-planet system typically of similar size? Perhaps the physics of planet formation set a size to which planets prefer to grow. We find a weak correlation between planet size and stellar mass in multi-planet systems, suggesting that stellar mass plays at most a minor role in determining planet sizes. *Thus, some property of the protoplanetary disk other than stellar mass influences the final planet sizes.* Furthermore, our brief examination here and a more detailed analysis by [Petigura et al. \(in preparation\)](#) do not find a strong correlation between stellar metallicity and planet size.

If stellar mass is not the dominant feature in determining planet sizes, we might think that perhaps the total disk mass from which the planets formed is a stronger predictor of planet size. [Andrews et al. \(2013\)](#) and [Pascucci et al. \(2016\)](#) noted that although there is a nearly linear correlation between stellar mass and disk mass, the disk mass varies by an order of magnitude for a

given stellar mass. Perhaps, if it were possible to measure, we might notice a strong correlation between disk mass and planet size for the sub-Neptune sized planets.

On the other hand, perhaps it is not disk mass, but some other aspect of planet formation that is most important in determining planet sizes. Other possible influences on the final planet sizes include the mass of solid material in the disk and the time at which the gas is depleted from the disk.

Although planets tend to be similar in size, the inner planet is smaller than the outer planet in 65% of adjacent pairs. The inner planet is smaller in 74% of pairs that straddle  $150 F_{\oplus}$ , but in only 58% of pairs where both planets receive less than  $150 F_{\oplus}$ . [Ciardi et al. \(2013\)](#) also found that, after correcting for detectability, the outer planet is larger than the inner planet in 68% of pairs, but this was only true for planets larger than  $3 R_{\oplus}$ . Restricting their sample to planets smaller than  $3 R_{\oplus}$ , they found no preference for smaller inner planets, whereas we do.

Asymmetry in adjacent planet sizes might arise from photoevaporation. In photoevaporation, stellar X-ray and Extreme UV (EUV) radiation photoionize the upper atmosphere of an exoplanet, causing it to heat and overflow the planet's Roche Lobe in a runaway process that can strip the volatile layers (especially hydrogen and helium) of  $10 M_{\oplus}$  planets in a few hundred Myr to a few Gyr, depending on whether the star has a high X-ray luminosity early in its life ([Lopez et al. 2012](#); [Owen & Wu 2013](#); [Zahnle & Catling 2017](#)).

One possible interpretation of the link between the observed distribution of planet sizes and the photoevaporation mechanism is as follows. For planets that straddle  $150 F_{\oplus}$  today, the inner planet received more photoionizing radiation at the time the disk cleared, and therefore had a higher mass-loss rate (assuming the planets were born with similar masses and densities). Therefore, more volatiles were stripped from the inner planet, resulting in a smaller size today. However, for pairs of planets beyond  $150 F_{\oplus}$ , the mass-loss rate of both planets was sufficiently low that very little volatile material was removed, and so the planets are likely to have similar sizes today.

Why are planets approximately 20 mutual Hill radii apart, with very few pairs closer than 10 mutual Hill radii? [Fang & Margot \(2012\)](#), [Pu & Wu \(2015\)](#), and [Dawson et al. \(2016\)](#) have also estimated that the *Kepler* planets have a typical spacing of about 20 mutual Hill radii, but our updated planet radii and stellar masses allow a more robust estimate.

The regular spacing of planets might be evidence that planets in systems with multiple transiting planets have been relatively undisturbed since their formation. Perhaps these systems formed *in situ*, at orbital distances

determined by their feeding zones, and grew to their present sizes based on the available material, as suggested in Goldreich et al. (2004), Lee & Chiang (2016), and Dawson et al. (2016).

Furthermore, the gas fraction in the nebular environment likely sculpted the sizes of the planets' feeding zones. Gas-rich disks damp eccentricities and keep feeding zones small, whereas gas-poor disks fail to damp eccentricities, allowing planetesimals to carve out larger feeding zones (Dawson et al. 2016). If the gas content of the disk affected the feeding zones of the planets, it likely also influenced their final compositions. The planetesimals embedded in gas-rich disks likely accreted more gas than planetesimals in gas-poor disks.

Therefore, if *in situ* formation is the dominant mode of planet formation, we expect the planets that formed in gas-rich environments likely have small mutual Hill separations and large ( $> 1\%$ ) gas fractions, whereas we expect the planets that formed in gas-poor disks likely have large mutual Hill separations and low ( $< 1\%$ ) gas fractions (Dawson et al. 2016). However, this prediction does not apply to planets whose gas fractions have been significantly depleted due to photoevaporation.

On the other hand, perhaps the Kepler planets experienced migration in a gas disk but were never caught in mean-motion resonances. The planets would need sufficiently low masses (compared to their stars) and sufficiently high eccentricities to escape resonant capture (Pan & Schlichting 2017). However, because the Type I migration rate scales with planet mass, the planet masses might need to be finely tuned to reproduce the observed regular spacing of planets. Furthermore, for many of the *Kepler* systems, the tight spacing ( $\Delta < 20$ ) requires low eccentricities for dynamical stability (Fang & Margot 2012; Pu & Wu 2015; Petrovich 2015; Dawson et al. 2016). The low eccentricities required for stability today might be inconsistent with the high eccentricities needed to escape capture in mean-motion resonance in the past.

Measurements of the masses and eccentricities of regularly spaced planets, especially in systems where photoevaporation has played at most a minor role, will test the predictions of *in situ* formation models and Type I migration models. Obtaining accurate planet multiplicity, planet masses, and planet orbital dynamics in such systems might elucidate how the majority of the *Kepler* sub-Neptune sized planets formed.

Since the TESS primary mission is expected to obtain at most a year of continuous photometry (in the continuous viewing zones Ricker et al. 2015), it will not be as sensitive to long-period planets in multi-planet systems as *Kepler* was. Additional planet searches using radial velocity data, transit follow-up, astrometry from Gaia, and direct imaging from WFIRST with a starshade will

help extend our sensitivity to as many planets as possible in multi-planet systems. Such observations are necessary to further test the predictions of planet formation theories.

The CKS project was conceived, planned, and initiated by AWH, GWM, JAJ, HTI, and TDM. Keck time for the CKS multis project was acquired by GWM, with assistance from LMW. The observations were coordinated by HTI and AWH and carried out by AWH, HTI, GWM, JAJ, TDM, BJF, LMW, EAP, ES, and LAH. AWH secured CKS project funding. SpecMatch was developed and run by EAP and SME@XSEDE was developed and run by LH and PAC. Downstream data products were developed by EAP, HTI, and BJF. Results from the two pipelines were consolidated and the integrity of the parameters were verified by AWH, HTI, EAP, GWM, with assistance from BJF, LMW, ES, LAH, and IJMC. EAP computed derived planetary and stellar properties with assistance from BJF. LMW performed the analysis in this paper, with assistance from GWM, JW, and AC. This manuscript was largely written by LMW with assistance from JW and GWM.

We thank John Asher Johnson, a PI and originator of the magnitude-limited CKS survey. Conversations with Jason Rowe, Scott Tremaine, and Jack Lissauer strongly influenced this paper. The results presented herein were made possible by observations at the W. M. Keck Observatory, which is operated as a scientific partnership among the California Institute of Technology, the University of California, and NASA. We are grateful to the time assignment committees of the University of Hawaii, the University of California, the California Institute of Technology, and NASA for their generous allocations of observing time that enabled this large project. Kepler was competitively selected as the tenth NASA Discovery mission. Funding for this mission is provided by the NASA Science Mission Directorate. L. M. W. acknowledges support from Gloria and Ken Levy and from the Trottier Family Foundation. E. A. P. acknowledges support from Hubble Fellowship grant HST-HF2-51365.001-A awarded by the Space Telescope Science Institute, which is operated by the Association of Universities for Research in Astronomy, Inc. for NASA under contract NAS 5-26555. B. J. F. acknowledges National Science Foundation Graduate Research Fellowship under Grant No. 2014184874. A. W. H. acknowledges NASA grant NNX12AJ23G. T. D. M. acknowledges NASA grant NNX14AE11G. P. A. C. acknowledges National Science Foundation grant AST-1109612. L. H. acknowledges National Science Foundation grant AST-1009810. E. S. is supported by a post-graduate scholarship from the Natural Sciences and Engineering



Research Council of Canada. Finally, the authors wish to recognize and acknowledge the very significant cultural role and reverence that the summit of Maunakea

has always had within the indigenous Hawaiian community. We are most fortunate to have the opportunity to conduct observations from this mountain.

## REFERENCES

- Andrews, S. M., Rosenfeld, K. A., Kraus, A. L., & Wilner, D. J. 2013, *ApJ*, 771, 129
- Ballard, S., & Johnson, J. A. 2016, *ApJ*, 816, 66
- Borucki, W. J., Koch, D. G., Brown, T. M., et al. 2010, *ApJL*, 713, L126
- Brown, T. M., Latham, D. W., Everett, M. E., & Esquerdo, G. a. 2011, *The Astronomical Journal*, 142, 112
- Carter, J. A., Agol, E., Chaplin, W. J., et al. 2012, *Science*, 337, 556
- Chen, J., & Kipping, D. 2017, *ApJ*, 834, 17
- Christiansen, J. L., Jenkins, J. M., Caldwell, D. A., et al. 2012, *PASP*, 124, 1279
- Ciardi, D. R., Fabrycky, D. C., Ford, E. B., et al. 2013, *The Astrophysical Journal*, 763, 41
- Dawson, R. I., Lee, E. J., & Chiang, E. 2016, *ApJ*, 822, 54
- Fabrycky, D. C., Lissauer, J. J., Ragozzine, D., et al. 2014, *ApJ*, 790, 146
- Fang, J., & Margot, J.-L. 2012, *ApJ*, 761, 92
- Furlan, E., Ciardi, D. R., Everett, M. E., et al. 2017, *AJ*, 153, 71
- Gladman, B. 1993, *Icarus*, 106, 247
- Goldreich, P., Lithwick, Y., & Sari, R. 2004, *Annual Review of Astronomy and Astrophysics*, 42, 549
- Hansen, B. M. S., & Murray, N. 2013, *The Astrophysical Journal*, 775, 53
- Johnson, J. A., Petigura, E. A., Fulton, B. J., et al. 2017, *ArXiv e-prints*, arXiv:1703.10402
- Latham, D. W., Rowe, J. F., Quinn, S. N., et al. 2011, *ApJL*, 732, L24
- Lee, E. J., & Chiang, E. 2016, *The Astrophysical Journal*, 817, 90
- Lissauer, J. J., Ragozzine, D., Fabrycky, D. C., et al. 2011, *ApJS*, 197, 8
- Lissauer, J. J., Marcy, G. W., Rowe, J. F., et al. 2012, *ApJ*, 750, 112
- Lissauer, J. J., Marcy, G. W., Bryson, S. T., et al. 2014, *ApJ*, 784, 44
- Lopez, E. D., Fortney, J. J., & Miller, N. 2012, *ApJ*, 761, 59
- Marcy, G. W., Isaacson, H., Howard, A. W., et al. 2014, *The Astrophysical Journal Supplement Series*, 210, 20
- Mullally, F., Coughlin, J. L., Thompson, S. E., et al. 2015, *The Astrophysical Journal Supplement Series*, 217, 31
- Owen, J. E., & Wu, Y. 2013, *ApJ*, 775, 105
- Pan, M., & Schlichting, H. E. 2017, *ArXiv e-prints*, arXiv:1704.07836
- Pascucci, I., Testi, L., Herczeg, G. J., et al. 2016, *ApJ*, 831, 125
- Petigura, E. A., Howard, A. W., Marcy, G. W., et al. 2017, *ArXiv e-prints*, arXiv:1703.10400
- Petrovich, C. 2015, *ApJ*, 805, 75
- Pu, B., & Wu, Y. 2015, *ApJ*, 807, 44
- Ricker, G. R., Winn, J. N., Vanderspek, R., et al. 2015, *Journal of Astronomical Telescopes, Instruments, and Systems*, 1, 014003
- Rogers, L. a. 2015, *ApJ*, 801, 41
- Rowe, J. F., Bryson, S. T., Marcy, G. W., et al. 2014, *ApJ*, 784, 45
- Steffen, J. H., & Hwang, J. A. 2015, *MNRAS*, 448, 1956
- Weiss, L. M., & Marcy, G. W. 2014, *ApJ*, 783, L6
- Weiss, L. M., Marcy, G. W., Rowe, J. F., et al. 2013, *The Astrophysical Journal*, 768, 14
- Wolfgang, A., & Lopez, E. 2015, *ApJ*, 806, 183
- Xie, J.-W., Dong, S., Zhu, Z., et al. 2016, *Proceedings of the National Academy of Science*, 113, 11431
- Zahnle, K. J., & Catling, D. C. 2017, *ArXiv e-prints*, arXiv:1702.03386